https://dx.doi.org/10.21577/0103-5053.20230037

J. Braz. Chem. Soc., Vol. 34, No. 9, 1262-1272, 2023

Article

Stable and Thermo-Responsive Dextran Sulfate-Graft-PNIPAm Amphiphilic Nanoparticles for Potential Target Methotrexate Delivery

Aline T. dos Santos,[a] Emerson L. da Silva,[b] Raquel C. Montenegro,[b] Jeanlex S. de Sousa,[c] Regina C. M. de Paula[a] and Judith P. A. Feitosa[,a]*

[a]*Laboratório de Polímeros, Departamento de Química Orgânica e Inorgânica, Centro de Ciências, Universidade Federal do Ceará, 60455-760 Fortaleza-CE, Brazil*

[b]*Núcleo de Pesquisa e Desenvolvimento em Medicamentos, Universidade Federal do Ceará, 60430-275 Fortaleza-CE, Brazil*

[c]*Departamento de Física, Centro de Ciências, Universidade Federal do Ceará, 60455-760 Fortaleza-CE, Brazil*

Thermo-responsive copolymers grafted with *N*-isopropylacrylamide (NIPAm) are excellent candidates for drug release. Dextran sulfate (DS) acts as a specific ligand in inflamed regions, turning it highly useful as a target for drug delivery. DS was associated with NIPAm to produce amphiphilic graft copolymers prepared via free radicals. The molar ratio of feed reagents NIPAm/DS varied from 1 (DS-*g*-PNIPAm) to 4 (DS-*g*-4PNIPAm). The synthesis was confirmed by spectroscopic techniques (Fourier transform infrared (FTIR) and nuclear magnetic resonance (NMR)). All copolymers showed self-organization capacity in an aqueous medium in temperatures higher than 34 °C, and sizes less than 300 nm. DS-*g*-3PNIPAm exhibited stability in water and in phosphate buffer at pH 7.4. Scanning electron microscopy confirmed their spherical shape. This copolymer showed specificity to leukemic cells, and normal cells' proliferation. Methotrexate (MTX) is a very low water-soluble drug used for rheumatoid arthritis and cancer. Unfortunately, MTX have severe collateral effects. MTX-loaded nanoparticles can overcome such issues as well as enhance bioactivity and stability. The MTX was encapsulated and delivered from the DS-*g*-3PNIPAm with potential target delivery due to the presence of DS. Comparison with MTX encapsulated in other nanoparticles reveals that the DS-*g*-PNIPam presents the best performance among the thermo-responsive and the second among the target MTX nanocarriers.

Keywords: nanocarriers, *N*-isopropylacrylamide, dextran sulfate, graft copolymers, cancer cell, methotrexate

Introduction

For most traditional delivery systems, the drug is administered based on the blood circulation system. However, generally, only a small portion of the drug reaches the target sites of the disease. For example, about 1% of the drugs administered will reach the tumor site in chemotherapy, while almost 99% will not, usually leading to side effects such as nausea, hair loss, and fatigue.[1]

In recent years, nanomedicine has stood out since it provides great potential to overcome difficulties in administering therapeutic agents in specific locations. Multifunctional materials can be developed to selectively concentrate drug molecules in a specific area through the effect of improved permeability and retention (IPR).[2] The term enhanced permeability and retention effect describe the unique pathophysiological phenomenon of solid tumor vasculature.[3] In this manner, these materials significantly enhance the efficiency of the treatment and reduce unwanted side effects.[4,5]

Polysaccharides represent a unique class of materials used, especially, in the preparation of pharmaceutical formulations as drug carriers, due to their biocompatibility, bioadhesiveness, and biodegradability.[6] These biomaterials' surfaces act as passive interfaces with the body (immune system, blood, cells) and actively participate in cell dissemination, proliferation, differentiation, and migration:

*e-mail: judith@dqoi.ufc.br
Editor handled this article: Fernando C. Giacomelli (Associate)

phenomena that are intensely linked to surface/cell interactions.[7]

Among the polysaccharides, dextran is a highly suitable candidate for chemical modification, besides being hydrophilic and biocompatible. In its sulfated form, the dextran sodium sulfate (DS), is a polyanionic biocompatible polymer, highly charged, and extremely water-soluble. Sulfated polysaccharides such as DS, fucoidan and carrageenan were initially thought to be macrophage scavenger receptor ligands.[8] In more recent time, *in vitro* and *in vivo* studies proved that DS was a ligand for the class A activated macrophage scavenger receptor (SR-A).[9-13] The SR-A receptor is mainly localized on the surface of activated macrophages present in inflamed regions. They are specifically recognized and bound by the anionic macromolecule.[12] Therefore, DS is highly useful as a target for drug delivery.

Amphiphilic copolymers have versatile properties that make them suitable for delivering hydrophilic and hydrophobic drugs.[14,15] Several polymers have been used to compose the side chains of amphiphilic copolymers. One of them is poly(*N*-isopropylacrylamide) (PNIPAm), a smart polymer that alters their structure and their physical-chemical properties in response to temperature. This polymer has been extensively studied in the biomedical field, mainly because it presents a phase transition close to the human body temperature (32-34 ºC).[16] As a result, thermoset hydrogels from PNIPAm are well-known to be used as drug carriers for cancer treatment. For example, Silva and co-workers[17] prepared a dual responsive graft of PNIPAm with dextran for the drug delivery of doxorubicin. And these hydrogels were also used to administer 5-fluorouracil and metformin.[18]

Methotrexate (MTX) is a recognized drug for psoriasis, rheumatoid arthritis, cancer, and Crohn's disease. However, MTX has some drawbacks that needs to be dealt with. For instance, this medication is toxic and in a high dose it can cause mucositis, myelosuppression, renal failure, hepatitis and necrotizing encephalopathy.[19] Other drawbacks of MTX that need to be mentioned is its very low water solubility (0.01 mg mL^{-1} at 20 °C), high sensitivity to heat and light, and quick degradation in the intestinal tract.[20] A strategy to overcome these aforementioned issues is by producing MTX-loaded nanoparticles which also favors the enhancement of its bioactivity and stability of the drug.[14]

There are some reports about MTX nanoparticles, but only two (as far as we known) studied the encapsulation of the drug with PNIPAm thermosensitive copolymers.[14,21] One of them is a block copolymers of poly(*N*-isopropylacrylamide)-*b*-poly(aspartic acid) nanomicelles developed for methotrexate encapsulation and delivery for ovarian cancer cell destruction.[14] These nanomicelles have a very low average zeta potential (–0.539 mV) and a high polydispersity index (PDI) of up to 0.5. These results indicate that these nanomicelles have low stability and a high heterogeneity of particle sizes, leading to the formation of precipitates. The other report concerns the use of PNIPAm-*g*-polyacrylic acid,[21] which has the disadvantage of low MTX release at 37 °C (less than 15%), requiring the use of a large amount of material to promote the delivery of MTX required for treatment. Few works report the synthesis of materials that present DS and MTX in their composition.[9-11] MTX was included in nanoparticles of β-cholanic acid conjugated with DS,[9] formed nanomicelles through DS-*g*-MTX grafting,[10] and in the modified form was linked to DS and loaded into double hydroxide layers.[11] Therefore, DS can be considered highly suitable as a target for MTX delivery.

Based on the above, this work aims to synthesize stable, self-organized and thermo-responsive dextran sulfate/*N*-isopropylacrylamide nanoparticles with potential target properties for MTX drug delivery with amount release > 50% at body temperature.

Experimental

Materials

Dextran sodium sulfate (DS) of molar mass 5×10^5 g mol^{-1} and degree of sulfation 2 was purchased from Serva (Heidelberg, Germany). *N*-Isopropylacrylamide (NIPAm), pyrene, potassium persulfate (KPS), and *N*,*N*,*N*',*N*'-tetramethylene-diamino (TEMED) were purchased from Sigma-Aldrich (Darmstadt, Germany). Acetone, anhydrous monopotassium phosphate, and disodium phosphate were purchased from Vetec (Duque de Caxias, Brazil). Sodium chloride, dimethyl sulfoxide, and sodium hydroxide were acquired from Synth (Diadema, Brazil). AlamarBlue was obtained from Merck (Darmstadt, Germany). Fetal bovine serum, penicillin, and streptomycin were purchased from Gibco (New York, USA).

Synthesis and purification of copolymers

The synthesis using the KPS initiator was based on the methodology described by Shi and Zhang,[22] with modifications. A mass of 500 mg of DS was dissolved in 100 mL of distilled water under a nitrogen atmosphere at 25 °C. Subsequently, the KPS with a 7:1 molar ratio (DS/KPS) was added, together with TEMED in a 1:1 molar ratio (KPS/TEMED). After 20 min, NIPAm was added to form the copolymer, and the system was maintained at room temperature in an inert atmosphere for 4 h. The resulting

solution was placed on dialysis against distilled water until the conductance of the residual water was close to that of the distilled water. After lyophilizing, the copolymers were dispersed in acetone under magnetic stirring for 24 h to dissolve the homopolymer that may have been formed. Finally, the copolymers were spun at 6000 rpm for 20 min. The precipitate was collected, redissolved in distilled water, and freeze-dried.

Four different syntheses were performed, varying the DS/NIPAm molar ratio from 1 to 4, obtaining the copolymers DS-*g*-PNIPAm, DS-*g*-2PNIPAm, DS-*g*-3PNIPAm, and DS-*g*-4PNIPAm. The number in front of the abbreviation PNIPAm means the theoretical number of moles of NIPAm added *per* mole of DS.

Fourier transform infrared spectroscopy (FTIR)

DS and the copolymers were analyzed in potassium bromide pellets in the spectrophotometer Shimadzu model IRTracer100 (Kyoto, Japan) in the region between 4000 and 400 cm^{-1}.

Nuclear magnetic resonance (NMR)

The analyses of the copolymers and PNIPAm by hydrogen nuclear magnetic resonance (^1H NMR) were performed in the Bruker Model Avance DRX500 equipment (Billerica, USA) at 25 ºC using as standard the 4,4-dimethyl-4-silapentane1-sulfonic acid (DSS). The samples were prepared in deuterated water (D_2O).

Dynamic light scattering (DLS)

The measurements were obtained by DLS with non-invasive countercurrent scattering (DLS-NIBS) in the range from 25 to 50 °C in 0.5 mg mL^{-1}. A red laser (633 nm) was applied to the sample with detection at an angle of 173°. The zeta potential of the copolymers was measured by laser Doppler velocimetry with light exchange phase analysis (M3-PALS). A Nanosizer ZS 3600 (Malvern Instruments Ltd, Worcestershire, United Kingdom) was used for both studies.

LCST is the lower critical solution temperature, at which occurs a phase transition. Below LCST, the PNIPAm chains are soluble in water due to the hydrogen bonds between the polymer (amide groups) and water molecules. Above the LCST, hydrogen bonds with water are not favored and the PNIPAm performs hydrogen bonds with groups similar to it, resulting in an expulsion of water molecules from the polymeric network, and a consequent formation of self-organized aggregates.[23] Based on this premise, the analysis was performed to determine the hydrodynamic diameter of the copolymers in aqueous solution as a function of temperature in the range of 25 to 50 °C. The particle size of the copolymers was analyzed at each 1 °C increase, with an equilibration time of 4 min before each analysis. The tests were performed in triplicate.

Stability study

The Z-average diameter and the polydispersity index were analyzed as parameters of stability of the nanoparticles.[24] These parameters were investigated in two conditions: (*i*) nanoparticles at 37 °C in 0.1 mol L^{-1} phosphate buffer (PBS) solution (pH 7.4) for a period of 72 h and (*ii*) at 4 °C in distilled water for 6 months. Both measurements were determined at 37 ºC in triplicate using 0.5 mg mL^{-1} copolymer solutions in the Malvern Nano Zetasizer model ZS 3600.

Morphology

The nanoparticles morphology was examined using scanning electron microscopy (SEM). SEM was performed on the equipment Quanta FEG 450-FEI (Hillsboro, USA) at a voltage of 20 kV. 20 µL of diluted samples of the copolymer in water (1:10 v/v) was left under stirring for 24 h. Subsequently, the solution was dripped onto the carbon strip and left to evaporate at 37 °C in an oven. The sample was covered with gold using the Metallizer Quorum QT150ES (Laughton, United Kingdom).

Cell culture

Two human cell lines were used: chronic myeloid leukemia (CML) K562 and the normal line derived from pulmonary fibroblast MRC5. The K562 strain was grown in RPMI medium (Roswell Park Memory Institute medium) and the MRC5 strain in DMEM medium (Eagle medium modified by Dulbecco), supplemented with 10% SBF (bovine fetal serum) and 1% antibiotics (penicillin/streptomycin 5000 U/5000 µg mL^{-1}), being kept in a culture oven with a 5% CO_2 atmosphere, at 37 ºC.

Cytotoxicity tests

Cytotoxicity was assessed using the fluorescent compound alamarBlue.[25] K562 and MRC5 cell lines were plated in 96-well plates at a concentration of 5×10^3 and 3×10^3 cells *per* well, respectively, and incubated in a CO_2 oven for 24 h. Then, treatment with the DS-*g*-3PNIPAm copolymer was performed in a serial dilution curve (200-3,125 µg mL^{-1}). The toxicity was evaluated after 72 h

by the addition of the fluorescent compound alamarBlue (0.2 mg mL^{-1}). The fluorescence (excitation 530 nm, emission 590 nm) was measured in a spectrophotometer (Beckman Coulter Microplate Reader DTX 880, Brea, USA), and the percentage of cell viability estimated.

The fluorescence of the untreated group (negative control) was equal to 100% of cell viability. The data were analyzed from the mean standard deviation of 3 independent experiments. To verify the occurrence of a significant difference between the groups, the data were compared by two-way analysis of variance (ANOVA) followed by a Bonferroni post-test, with a significance level of 95% ($p < 0.05$) using the GraphPad Prism® 6 statistical program.[26]

Incorporation and release of methotrexate

MTX was encapsulated in the DS-*g*-3PNIPAm copolymer by mixing 8 mL of 1 mg mL^{-1} copolymer solution with 2 mL of the drug solution at a 1 mg mL^{-1} concentration following the previous procedure.[27] The two solutions were prepared in dimethyl sulfoxide (DMSO). This copolymer/MTX solution was dripped into a 20 mL of 0.01 mol L^{-1} NaCl solution at 37 °C, maintained for 4 h under slow stirring to form the nanoparticles. Then, it was dialyzed against distilled water for 24 h to remove the DMSO and lyophilized.

The release profile of the nanoparticles loaded with MTX was obtained using a dialysis system. The nanoparticle containing MTX (10 mg) was dissolved in 3 mL of PBS 7.4, introduced into a cellulose acetate membrane (14,000 g mol^{-1}) and dialyzed against 20 mL of PBS buffer solution at pH 7.4 and 37 °C. Samples were removed at time intervals, and the extent of cumulative drug release determined by measuring absorbance at 302 nm by spectrophotometry.

The quantification of MTX in the nanoparticles was performed using DMSO for the extraction of the drug. This analysis was carried out in a SHIMADZU UV-1800 UV-visible spectrophotometer (Kyoto, Japan), by using the wavelength of 302 nm, which is characteristic of MTX. The calibration curve, with linear correlation coefficient, is:

$$ABS = 0.000982 + 53.35C \quad (1)$$

where ABS is the absorbance, and C is the concentration of MTX in mg mL^{-1}.

Results and Discussion

Grafting reaction of NIPAm onto dextran sulfate was shown in Figure S1, Supplementary Information (SI) section. The yield of these reactions was calculated using the following equation:

$$\text{Yield}(\%) = \frac{m_{DS-PNIPAm}}{m_{DS} + m_{NIPAm}} \times 100 \quad (2)$$

where $m_{DS-PNIPAm}$ is the mass of the purified grafts, after the elimination of homopolymer (PNIPAm); m_{DS} and m_{NIPAm} Are the mass of dextran sulfate and NIPAm monomer, respectively.

The yield of the grafting (wt.%) are 53.0 ± 0.9, 50.3 ± 1.2, 49.1 ± 1.4, and 39.7 ± 1.8 for DS-*g*-4PNIPAm, DS-*g*-3PNIPAm, DS-*g*-2PNIPAm and DS-*g*-PNIPAm, respectively. The decrease in the yield as NIPAm increase is probably due to higher amount of homopolymer obtained as monomer concentration increases.

The FTIR was obtained to analyze the structure of the copolymers and starting materials (Figure 1). The bands that confirm the presence of PNIPAm into the copolymers were 1544 cm^{-1} (δN–H) and 1468 cm^{-1} (δC–N). The presence of DS was confirmed through the signals at 1257 cm^{-1} (νS=O), 1016 cm^{-1} (ν_sC–O–C of glycosidic bond), 985 cm^{-1} (νS=O) and 822 cm^{-1} (νO–S–O).[28] The absorption band at 3508 cm^{-1} (νO–H) is attributed mainly to hydroxyl groups from polysaccharide, at 2949 cm^{-1} (ν_{ass}C–H of CH_2), and 1653 cm^{-1} is assigned to moisture. In PNIPAm, the bands at 2971 and 1651 cm^{-1} are associated with the νC–H of the isopropyl group and with the νC=O bond of the amide group (–CONH–) (amide I), respectively. The band at 1544 cm^{-1} is attributed to the N–H deformation vibration of the amide group and 1468 cm^{-1} to the C–N angular deformation.[29]

The ^{1}H NMR spectra of homo and copolymers were shown in Figure 2. The analysis was conducted at 25 ºC,

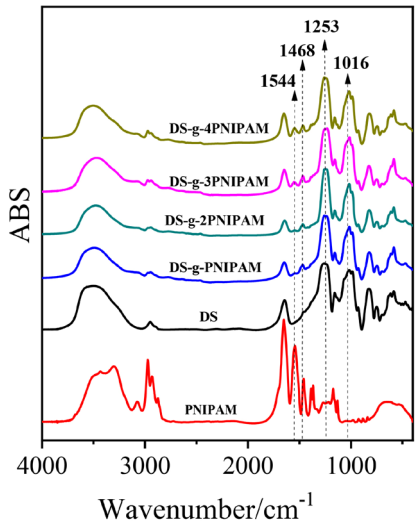

Figure 1. FTIR (KBr) spectra of start materials and copolymers.

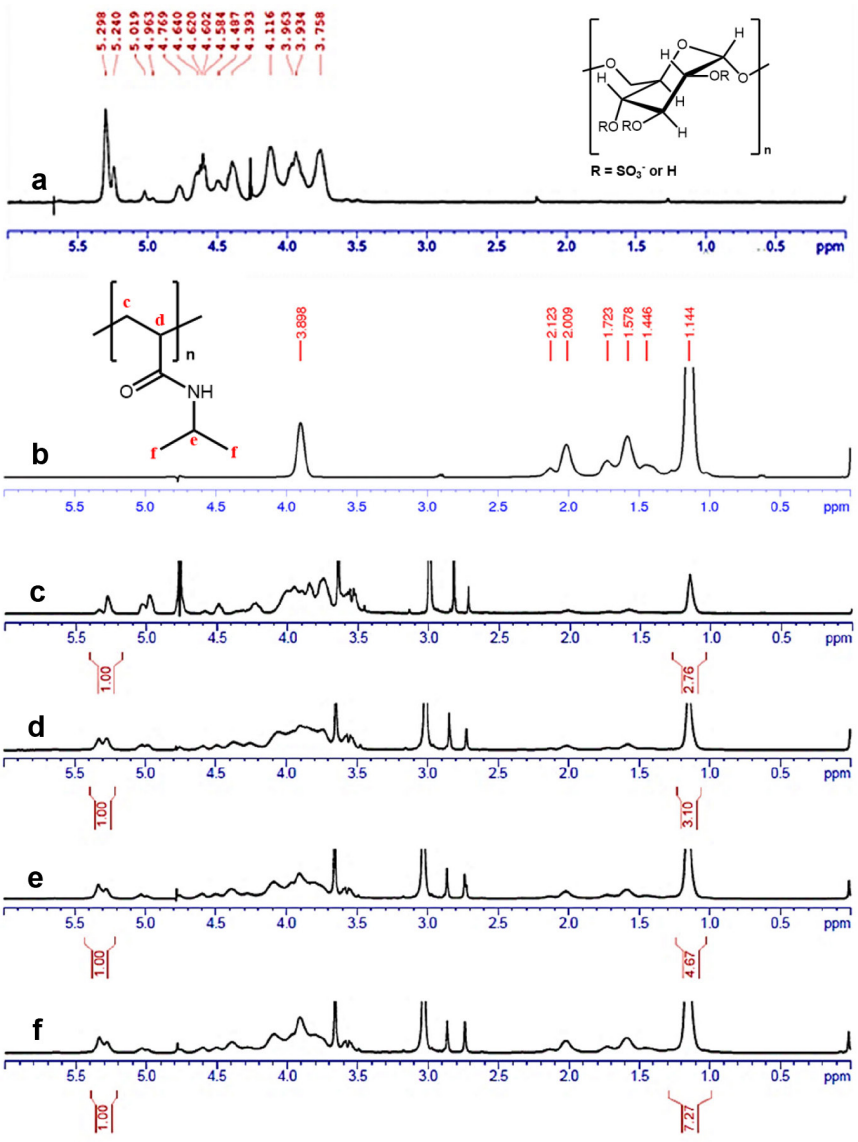

Figure 2. ^{1}H NMR spectra of DS (a), PNIPAm (b), DS-*g*-1PNIPAm (c), DS-*g*-2PNIPAm (d), DS-*g*-3PNIPAm (e) and DS-*g*-4PNIPAm (f).

temperature much smaller than the expected LCST (around 34 ºC). In temperature higher than LCST, the hydrophobic segments of PNIPAm contract with the formation of the nucleus. The hydrophilic part of polysaccharide would act as a shell, covering the nanoparticle, making it difficult to perceive the PNIPAm structure groups' signals. Similar behavior was also observed for cashew gum-*g*-PNIPAm copolymers.[29]

The signals from 5.5 to 3.5 ppm for copolymers are attributed to the DS bound to PNIPAm.[30] The presence of PNIPAm was confirmed by the hydrogens at 3.89 (–C*H*(CH_3)$_2$) (Figure 2e), 2.06 (–C*H*–CH_2) (Figure 2c), 1.58 (–CH–C*H*$_2$) (Figure 2d) and 1.14 ppm (–CH(C*H*$_3$)$_2$) (Figure 2f). These were also observed for double brush-shaped PNIPAm graft.[31] The signal at 4.75 ppm refers to residual solvent (H_2O).

The PNIPAm/DS molar ratio was determined from the ratio of the signal areas corresponding to the protons of the isopropyl group (–CH (C*H*$_3$)$_2$) of PNIPAm in 1.14 ppm (Figure 2f) and the signal relative to the anomeric proton of the α-1,6 bond between 5.3 and 5.4 ppm (equation 3).

$$\text{PNIPAm / DS} = \frac{\text{NIPAM}}{\text{AGU}} = \frac{\text{area at 1.14 ppm} \,/\, 6}{\text{area at 5.3} - \text{5.4 ppm}} \quad (3)$$

NIPAM is the number of moles of the acrylic monomer, and AGU is the number of moles of the anhydrous glycosidic unit.

The molar ratios of the copolymers calculated by equation 3 were 0.46, 0.56, 0.78, and 1.21 for DS-*g*-1PNIPAm, DS-*g*-2PNIPAm, DS-*g*-3PNIPAm and DS-*g*-4PNIPAm, respectively. The PNIPAm content

increased from 12.4 wt.% for DS-*g*-1PNIPAm, to 46.2 wt.% for DS-*g*-4PNIPAm. Three chemical shifts attributed to PNIPAm (hydrogens c, d, and f) can be seen in copolymers' spectra in Figure 2. The displacement referring to hydrogen e was not observed because it is superimposed to the DS signals.

The effect of temperature on the hydrodynamic diameter was performed by DLS technique. Dextran sulfate, as expected, did not show phase transition. PNIPAm presents LCST at 34 °C, which increases hydrodynamic diameter after this temperature (Figure 3). This increase is not due to dehydration only, but to the formation of aggregates during/after water loss. All grafts showed LCST slightly higher and decrease in diameter after then. In these cases, due to negative surface electrical charge, the repulsion avoids the aggregates formation and increasing diameter. The same behavior was reported with PNIPAm grafted into polyacrylic acid,[21] and with galactomannan.[27] There is no formation of aggregates. So, LCST is only due to water loss.

Data obtained from DLS are shown in Table 1. All synthesized copolymers formed nanoparticles when heated, proving the thermo-responsiveness of these materials. No trend can be observed between LCST and PNIPAm wt.%. The points below LCST are very disperse (Figure 3). In addition, the temperature variation interval was 1 °C, making the determination with low accuracy (± 1 °C), and impossible to see any trend. This is likely due to the heterogeneity of the monomer composition in the copolymers, arisen from the conventional free radical polymerization method.[32]

The PDI from DLS of DS-*g*-PNIPAm and DS-*g*-2PNIPAm showed higher values, giving more

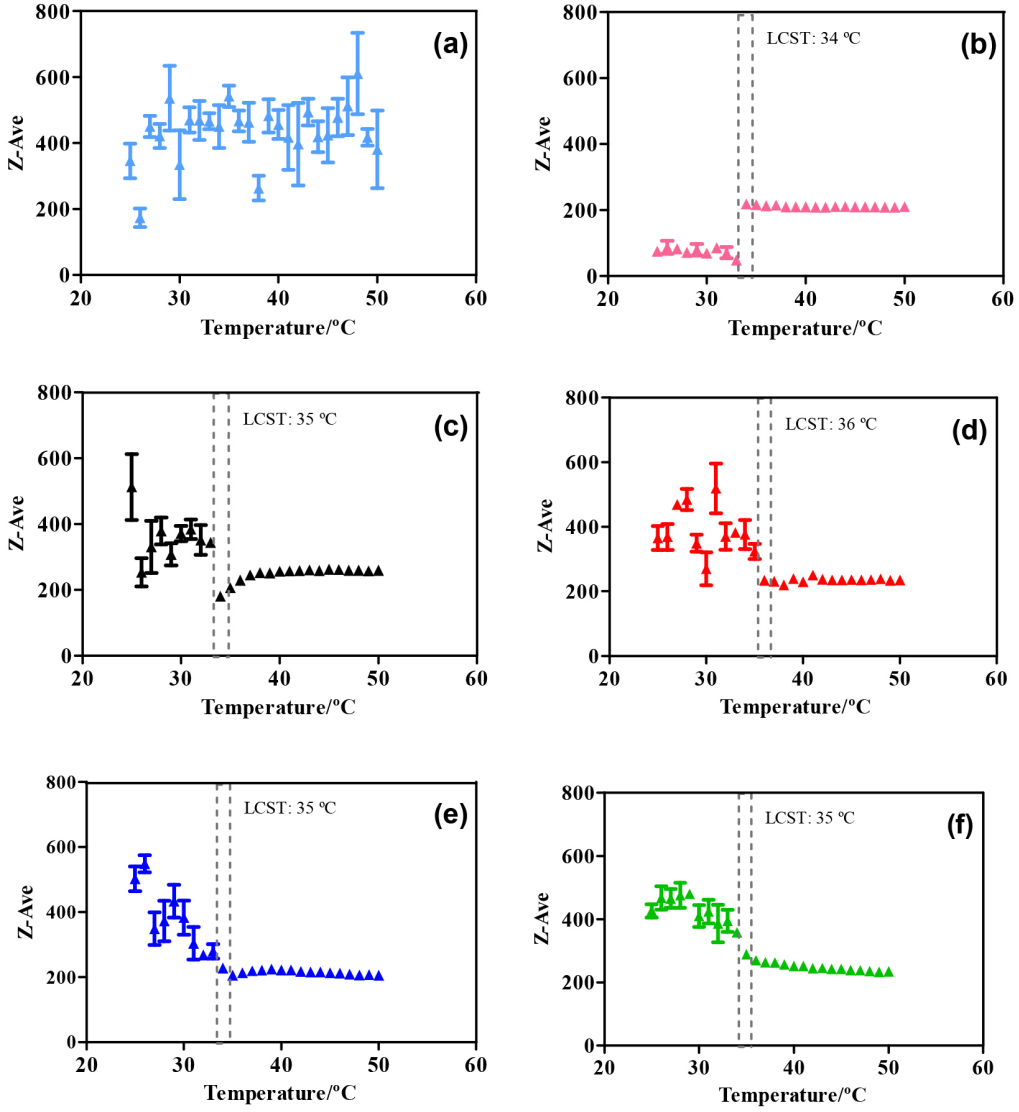

Figure 3. Effect of temperature over the particle size of the starting materials and copolymers: (a) DS; (b) PNIPAm; (c) DS-*g*-PNIPAm; (d) DS-*g*-2PNIPAm; (e) DS-*g*-3PNIPAm and (f) DS-*g*-4PNIPAm.

Table 1. Properties of self-organized copolymers, PNIPAm nanoparticles and DS

Nanoparticle	PNIPAm / wt.%	LCST / °C	Diameter[a] / nm	PDI	Zeta potential / mV
DS	–	–	463 ± 59	0.66 ± 0.11	–38.8 ± 5.4
PNIPAm	–	34 ± 1	214 ± 1	0.04 ± 0.01	–
DS-*g*-PNIPAm	12.4 ± 0.6	34 ± 1	245 ± 1	0.27 ± 0.01	–42.1 ± 4.3
DS-*g*-2PNIPAm	30.8 ± 0.6	36 ± 1	231 ± 6	0.31 ± 0.01	–39.5 ± 2.2
DS-*g*-3PNIPAm	40.7 ± 1.0	35 ± 1	218 ± 4	0.15 ± 0.01	–44.7 ± 2.5
DS-*g*-4PNIPAm	46.2 ± 0.9	35 ± 1	263 ± 1	0.17 ± 0.01	–40.5 ± 1.7

[a]Diameter (Z-average size) and zeta potential measured at 37 °C. DS: dextran sulfate; PNIPAm: poly(*N*-isopropylacrylamide); LCST: lower critical solution temperature; PDI: polydispersity index.

significant heterogeneity (Table 1). However, the PDI of DS-*g*-3PNIPAm and DS-*g*-4PNIPAm were small, 0.15 and 0.17, respectively, indicating good homogeneity, which favors application as a drug carrier. Taking into account the low value of PDI, and higher NIPAm%, DS-*g*-3PNIPAm and DS-*g*-4PNIPAm were chosen for further characterization. For drug release in a specific location, a range of 50 to 300 nm is preferred, especially for chemotherapy agents. Nanoparticles with this size provide better penetration of barriers, greater uptake in cells and rapid action.[33] Thus, DS-*g*-3PNIPAm and DS-*g*-4PNIPAm, with respective diameters of 218 and 263 nm, have the potential to be used as nanocarriers of chemotherapy drugs.

The physical-chemical stability of amphiphilic copolymer nanoparticles is vital for their biological applications, directly affecting the drug's absorption and physiological distribution.[34] Therefore, two tests were carried out: the first, in PBS, pH 7.4 at 37 °C for 72 h; and the second, in water at 4 °C for 6 months (Figure 4). The first simulates the circulation time of a drug in a physiological medium, and the second simulates the stability in the fridge. The negative values of zeta potential (ZP) justify the stability of the nanoparticle. The magnitude of ZP gives a prediction of the colloidal stability. ZP of nanoparticles (NPs) with values > + 25 mV or < –25 mV usually have high degree of stability. Lower ZP values will lead to aggregation, coagulation, or flocculation due to van der Waals interparticle attraction.[35]

The low variation of the average diameter of DS-*g*-3PNIPAm and DS-*g*-4PNIPAm in PBS indicated excellent stability during the analyzed period (Figure 4a). This is probably due to the high PNIPAm content and dimension homogeneity. Analyzing the second test data (Figure 4b), DS-*g*-3PNIPAm demonstrated high stability, but some variation was observed for DS-*g*-4PNIPAm. The particle size distributions over the 6-month period can be seen in Figure S3 (SI section).

Based on the results obtained on the stability of the copolymers, DS-*g*-3PNIPAm was chosen for the studies described below.

Differential scanning calorimetry (DSC) technique was used to study graft details (Figure 5). The three curves are completely different, in events temperature and enthalpy. In DSC curve of DS (Figure 5a), an exothermic event, referring to the crystallization temperature (Tc), occurs at 236 °C, with enthalpy (ΔH) = –129 J g^{-1}. The endothermic event, at 260 °C with ΔH = +96 J g^{-1}, is associated with the melting temperature (Tm). This suggested that the DS used in this study was semicrystalline.[28]

For the DS-*g*-3PNIPAm copolymer, the Tc and Tm were 207 °C (ΔH = –188 J g^{-1}) and 281 °C (ΔH = +142 J g^{-1}),

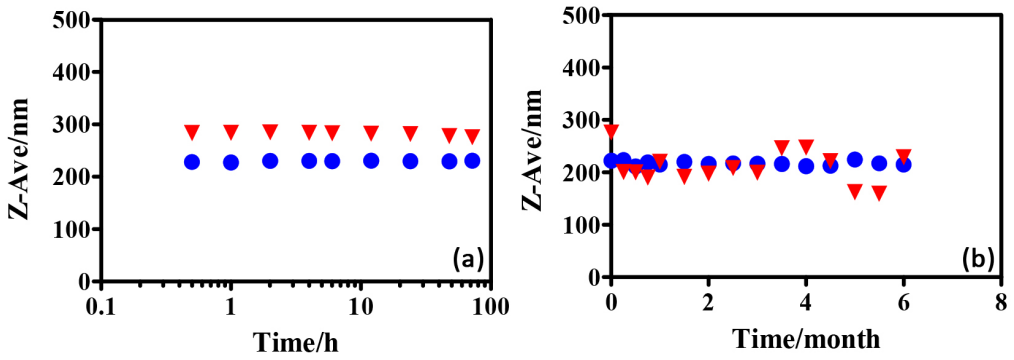

Figure 4. Stability of DS-*g*-3PNIPAm (●) and DS-*g*-4PNIPAm (▼) copolymers: (a) in phosphate buffer pH 7.4 at 37 °C for 72 h; (b) in aqueous solution at 4 ºC for 6 months, measurement performed at 37 ºC.

respectively. The endothermic event has a shift to higher temperatures and greater enthalpy change with the introduction of the PNIPAm. This causes an increase in interaction and greater organization of polymer chains, promoting an increase in the energy needed to melt the copolymer, when compared to DS. The PNIPAm curve showed an event at 408 °C, absent in the DS or copolymer curves.

The micrograph obtained by SEM (Figure 6a) and the histogram (Figure 6b) show that the nanoparticles have a spherical shape and their relative average size (120 nm) is significantly smaller than that obtained by DLS (218 nm). In SEM, the nanoparticles are in the absence of water, facilitating more significant interaction between the hydrophobic domains, causing this size reduction. By DLS, the analysis is performed in an aqueous solution, which favors an increase in interactions between surfaces, molecules, and ions, leading to the creation of adsorbed layers, causing an increase in size.[36]

The cytotoxicity analyses of the DS/PNIPAm copolymer were tested in the (leukemic cell) chronic myelogenous leukemia-K562 and (non-cancer cells) fibroblast-like fetal lung-MRC5 (Figure 7). The concentration range analyzed allows the evaluation of cytotoxicity without interference from other death mechanisms because the presence of sulfate groups and high concentrations can generate an ionic imbalance and promote death.[37]

After 72 h, a reduction in the viability of K562 and relative cell growth of MRC5 in the concentration range analyzed were observed, confirming the specificity of this copolymer. The lack of cytotoxicity in non-cancer cells and the reduced viability in cancer cells make this copolymer a potential candidate as a nanodrug carrier targeting leukemia cells.

As a proof of concept, the DS-*g*-3PNIPAm copolymer was loaded with a chemotherapeutic. MTX was used as a hydrophobic model drug. Encapsulation efficiency (EE) and drug content (DC) were determined by using equations 4 and 5:

$$EE\,(\%) = \frac{m_{ex}}{m_i} \times 100 \quad (4)$$

$$DC\,(\%) = \frac{m_{ex}}{m_{cop}} \times 100 \quad (5)$$

where m_{ex} is the mass of the nanoparticle's extracted drug; m_i is the initial mass of drug; m_{cop} is the mass of the copolymer.

The encapsulation efficiency was 27.6 ± 3.6% and the drug content 5.7 ± 0.6%. The values observed by Blanco-Fernandes *et al.*[37] for dextran-*g*-PNIPAm (EE 27.9%, DC 5.6%) at similar pH are close to the DS-*g*-PNIPAm results. Outstanding DC value of 88.3% was recently reported by Wang *et al.*[38] for MTX loaded into an acetalated dextran. However, the encapsulated efficiency was low (18.4%). Lowest values were obtained by Tu *et al.*[39] for PNIPAm-*co*-poly(L-lysine) (EE 12.7-20.1%,

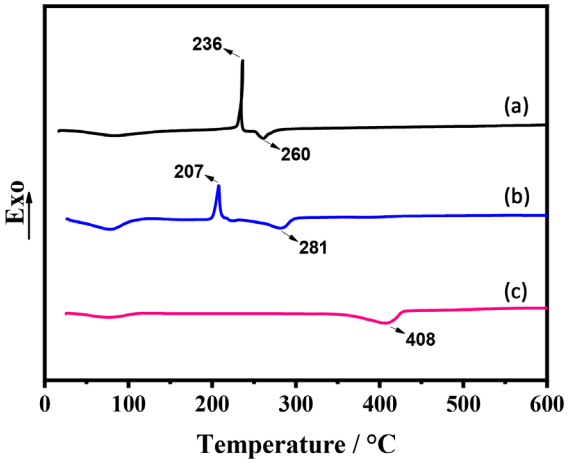

Figure 5. DSC curves for: (a) dextran sulfate, (b) DS-*g*-3PNIPAm copolymer, and (c) PNIPAm.

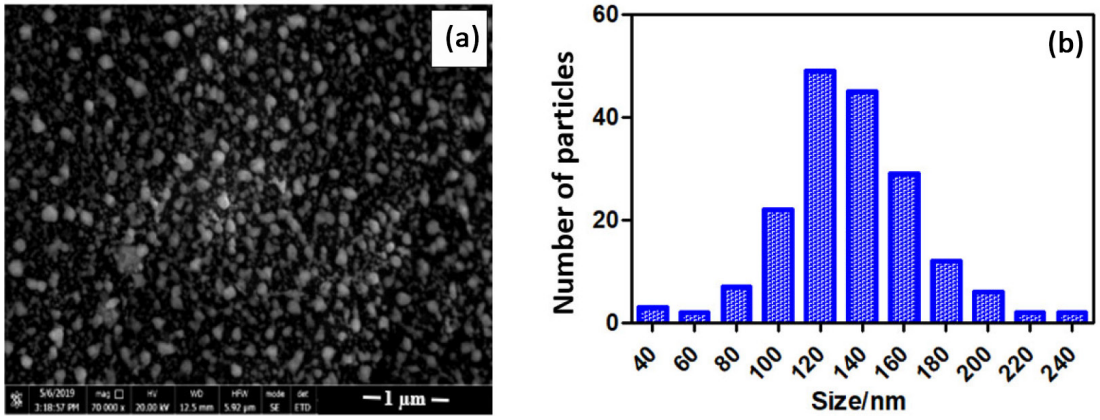

Figure 6. SEM micrographs for the nanoparticles: (a) DS-*g*-3PNIPAm and (b) histograms of the relative sizes of the nanoparticles.

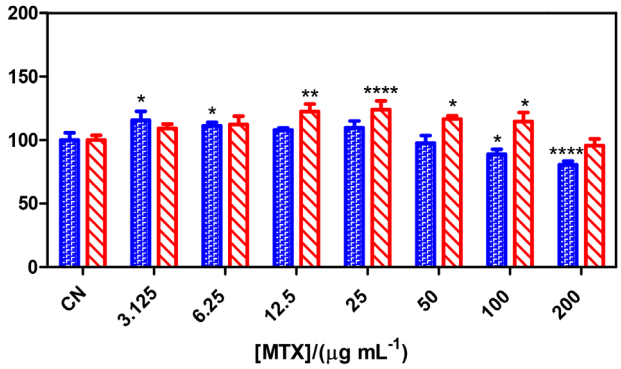

Figure 7. Cell viability of the leukemic strain K562 in blue (■) and the normal strain MRC5 in red (■) at 72 h. The bars represent the mean ± standard deviation of the mean of 3 independent experiments. *$p < 0.05$, **$p < 0.01$, ***$p < 0.001$ and ****$p < 0.0001$ when comparing cells without treatment (CN). The comparison was performed by two-way ANOVA followed by the Bonferroni test, with a significance level of 95% ($p < 0.05$).

DC 0.84-1.28%). The EE and DC for DS-*g*-PNIPAm can be considered as acceptable.

The MTX release from the DS-*g*-3PNIPAm in PBS 7.4 at 37 °C can be observed in Figure 8a. The burst release amounts is about 40% in the first 5 h, but the drug released reached 83 ± 5% after 72 h.

The behavior of DS-*g*-PNIPAm in relation to encapsulation and release of MTX can be compared to that of other nanoparticles containing DS or PNIPAm and MTX (Table 2). According to Blanco-Fernandes *et al.*,[37] the best NP size range for pharmaceutical use is 50-300 nm. Therefore, magnetic PNIPAm-*co*-polyacrylic acid,[21] and PNIPAm-*co*-poly(L-lysine)[39] are outside this range.

Considering 100 mg of NP, it is possible to calculate the mass of MTX that is released, just multiplying DC by release/100. Even taking into account all thermos-responsive systems, the mass of MTX released from all of them (1.24,[39] 1.86,[21] and 3.3[37] mg) is lower than that of DS-*g*-PNIPAm (4.5 mg released).

For the nanocarriers without PNIPAm, the mass released is 12.8,[12] 11.5,[38] 6.6.[10] Based on this parameter, DS-layered double hydroxide (12.8 mg),[12] MTX-acetalated dextran (11.5 mg),[38] and DS-cholanic acid (6.6. mg)[10] are better than the DS-*g*-PNIPAm.

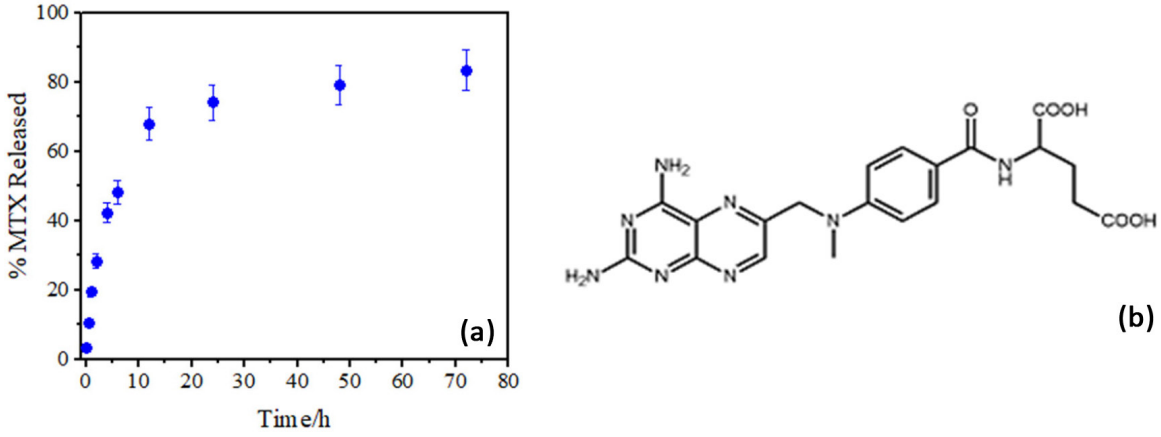

Figure 8. In (a) release of methotrexate from DS-*g*-PNIPAm graft; (b) chemical structure of MTX.

Table 2. Comparison among nanoparticle characteristics and MTX release from different systems containing DS or PNIPAm

System	NP characteristics			MTX			Reference
	Z-ave[a] / nm	PDI	Potential ζ / mV	EE / %	DC / %	Release[b] / %	
DS-cholanic acid	173	n.i.	–43.6	73.0	7.3	90	9
DS-*g*-MTX	100	n.i.	n.i.	n.i.	n.i.	n.i.	10
DS-layered double hydroxide	303	n.i.	–12.4	49.6	16.8	76	11
MTX-acetalated dextran	268	0.30	–20.3	18.4	88.3	13	36
PNIPAm-*co*-polyaspartic acid	65	< 0.5	–1.89	77.0	n.i.	65	13
Dextran-*g*-PNIPAm	88	n.i.	–16.6	27.9	5.6	59	35
Magnetic PNIPAm-*co*-polyacrylic acid	18	n.i	n.i.	41.3	37.2	5	20
PNIPAm-*co*-poly(L-lysine)	34	0.17	n.i.	12.7	1.3	95	37
DS-*g*-PNIPAm	218	0.15	–44.7	27.6	5.7	79	the present work

[a]Z-average size; [b]drug release at pH 7.4, 37 °C, 48 h. NP: nanoparticles; MTX: methotrexate; PDI: polydispersity index; EE: encapsulation efficiency; DC: drug content; DS: dextran sulfate; PNIPAm: poly(*N*-isopropylacrylamide); n.i.: not informed.

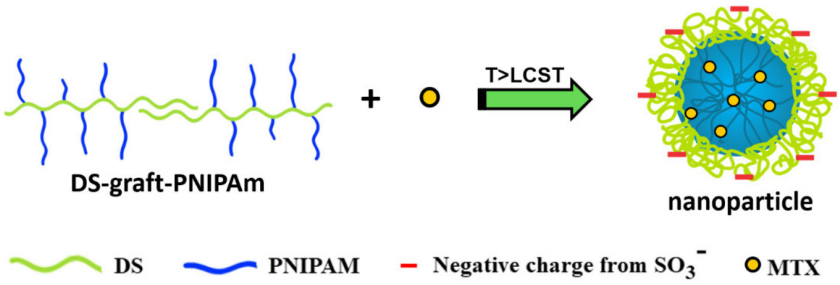

Figure 9. Proposed nanoparticle architecture.

The MTX-acetalated dextran nanosystem does not contain DS and did not present the target property. The two remaining systems (DS-layered double hydroxide,[12] and DS-cholanic acid[10]) show target behavior and higher released mass. Therefore, they are very good systems for encapsulating and releasing MTX. However, DS-*g*-PNIPam has a differential, which is its proven stability up to 72 h. DS-cholanic acid[10] had its stability tested only up to 12 h, but it is certainly stable for a longer time, since its ZP is –43.6 mV. The stability of the DS-layered double hydroxide system,[12] has not been reported, and is not expected considering the low ZP (–12.4 mV) presented.

It can be concluded that the DS-*g*-PNIPam presents the best performance among the thermo-responsive (with PNIPAm) and the second among the target (with DS) MTX nanocarriers.

The proposed architecture of the nanoparticle at a temperature higher than LCST (34 °C) can be seen in Figure 9. The outer layer of DS was based on the zeta potential and is similar to that proposed for DS-cholanic acid, whose zeta potential is comparable to that of DS-*g*-PNIPAm. The PNIPAm chains are hydrophobic and are located inside the NP, where the hydrophobic MTX molecules are also located.

Conclusions

Copolymers of DS with PNIPAm were successfully prepared by grafting via free radicals. As the molar relationship between the monomers is altered, structural changes occur. Nanoparticles of a more hydrophobic character was produced through the increase in temperature, confirming the thermo-responsiveness of the systems. The copolymers DS-*g*-3PNIPAm and DS-*g*-4PNIPAm showed specificity to leukemic cells, causing death in concentrations of 100 and 200 μg mL^{-1} and non-cancer cells' proliferation, reinforcing the importance of these nanocarriers in the drug encapsulation for the treatment of cancer. As a proof of concept, the hydrophobic drug methotrexate was encapsulated in DS-*g*-3PNIPAm and 79% released after 48 h. Comparison with MTX encapsulated in other nanoparticles reveals that the DS-*g*-PNIPam presents the best performance among the thermo-responsive and the second among the target MTX nanocarriers. The therapeutic potential of the model drug in cancer cells could be increased, considering that the vehicle itself has an effect on these cells.

Supplementary Information

Supplementary data are available free of charge at http://jbcs.sbq.org.br as PDF file.

Acknowledgments

The authors acknowledge and thank the financial support of the Brazilian agencies INOMAT-INCT, CNPq, CAPES, and FUNCAP, also to CENAUREM and the Central Analytica of the Federal University of Ceará (UFC), for the NMR and SEM analyses, and to the Laboratory of Pharmaceutical Genetics (NPDM), for the cytotoxicity tests.

Author Contributions

A. T. dos Santos was responsible for conceptualization, investigation, formal analysis, writing original draft, copolymers synthesis and characterization; E. L. da Silva and R. C. Monteiro for cytotoxicity investigation; J. S. de Sousa for microscopic investigation; R. C. M de Paula for conceptualization, funding acquisition; J. P. A. Feitosa for conceptualization, funding acquisition, project administration, writing-review and editing.

References

1. Wang, Y.; Khan, A.; Liu, Y.; Feng, J.; Dai, L.; Wang, G.; Alam, N.; Tong, L.; Ni, Y.; *Carbohydr. Polym.* **2019**, *223*, 115061. [Crossref]
2. Wu, J.; *J. Pers. Med.* **2021**, *11*, 771. [Crossref]
3. Matsumura, Y.; Maeda, H.; *Cancer Res.* **1986**, *46*, 6387. [Crossref]
4. Hou, M.; Gao, Y.; Shi, X.; Bai, S.; Ma, X.; Li, B.; Xiao, B.; Xue, P.; Kang, Y.; Xu, Z.; *Acta Biomater.* **2018**, *77*, 228. [Crossref]

5. Wu, D.; Li, Y.; Yang, J.; Shen, J.; Zhou, J.; Hu, Q.; Yu, G.; Tang, G.; Chen, X.; *ACS Appl. Mater. Interfaces* **2017**, *9*, 44392. [Crossref]
6. Cheaburu-Yilmaz, C. N.; Yilmaz, O.; Kose, F. A.; Bibire, N.; *Polymers* **2019**, *11*, 1432. [Crossref]
7. Conzatti, G.; Cavalie, S.; Combes, C.; Torrisani, J.; Carrere, N.; Tourrette, A.; *Colloids Surf., B* **2017**, *151*, 143. [Crossref]
8. Krieger, M.; Herz, J.; *Annu. Rev. Biochem*. **1994**, *63*, 601. [Crossref]
9. Kim, S.-H.; Kim, J.-H.; You, D. G.; Saravanakumar, G.; Yoon, H. Y.; Choi, K. Y.; Thambi, T.; Deepagan, V. G.; Jo, D.-G.; Park, J. H.; *Chem. Commun.* **2013**, *49*, 10349. [Crossref]
10. Heo, R.; You, D. G.; Um, W.; Choi, K. Y.; Jeon, S.; Park, J. S.; Choi, Y.; Kwon, S.; Kim, K.; Kwon, I. C.; Jo, D.-G.; Kang, Y. M.; Park, J. H.; *Biomaterials* **2017**, *131*, 15. [Crossref]
11. Yang, M.; Chang, F.; Ding, J.; Wang, J.; Gao, Z.; Zhuang, X.; Chen, X.; *J. Controlled Release* **2017**, *259*, e98. [Crossref]
12. Wang, X.; Yang, B.; Xu, X.; Su, M.; Xi, M.; Yin, Z.; *Drug Delivery Transl. Res.* **2021**, *11*, 1096. [Crossref]
13. Yu, C.; Liu, H.; Guo, C.; Chen, Q.; Su, Y.; Guo, H.; Hou, X.; Zhao, F.; Fan, H.; Xu, H.; Zhao, Y.; Mu, X.; Wang, G.; Xu, H.; Chen, D.; *Drug Delivery* **2022**, *29*, 454. [Crossref]
14. Pantshwa, J.; Choonara, Y. E.; Kumar, P.; du Toit, L. C.; Penny, C.; Pillay, V.; *J. Drug Delivery Sci. Technol.* **2017**, *39*, 308. [Crossref]
15. Qiao, P.; Niu, Q.; Wang, Z.; Cao, D.; *Chem. Eng. J.* **2010**, *159*, 257. [Crossref]
16. Yanase, K.; Buchner, R.; Sato, T.; *Phys. Rev. Mater.* **2018**, *2*, 085601. [Crossref]
17. Carneiro, M. J. M.; Paula, C. B. A.; Ribeiro, I. S.; de Lima, L. R. M.; Ribeiro, F. O. S.; Silva, D. A.; Araújo, G. S.; Marinho Filho, J. D. B.; Araújo, A. J.; Freire, R. S.; Feitosa, J. P. A.; de Paula, R. C. M.; *Int. J. Biol. Macromol.* **2021**, *185*, 390. [Crossref]
18. Wen, Y.; Liu, Y.; Zhang, H.; Zou, M.; Yan, D.; Chen, D.; Zhao, Y.; *Nanoscale* **2019**, *11*, 2687. [Crossref]
19. Salaün, H.; le Nail, L. R.; Simon, C.; Narciso, B.; de Pinieux, G.; Vegas, H.; Vinceneux, A.; *J. Oncol. Pharm. Pract.* **2022**, *28*, 1458. [Crossref]
20. Yu, W.-J.; Huang, D.-X.; Liu, S.; Sha, Y.-L.; Gao, F. H.; Liu, H.; *Front. Oncol.* **2020**, *10*, 1734. [Crossref]
21. Amantea, B. E.; Piazza, R. D.; Chacon, J. R.; Santos, C. C.; Costa, T. P.; Rocha, C. O.; Brandt, J. V.; Godoi, D. R. M.; Jafelicci Jr., M.; Marques, R. F. C.; *Colloids Surf., A* **2019**, *575*, 18. [Crossref]
22. Shi, H. Y.; Zhang, L. M.; *Carbohydr. Polym.* **2007**, *67*, 337. [Crossref]
23. Sliwa, T.; Jarzebski, M.; Gapinski, J.; Grzeszkowiak, M.; Kleshchanok, D.; *Acta Phys. Pol., A* **2014**, *125*, 1236. [Crossref]
24. Hou, X.; Zhang, W.; He, M.; Lu, Y.; Lou, K.; Gao, F.; *Asian J. Pharm. Sci.* **2017**, *12*, 558. [Crossref]
25. Rampersad, S. N.; *Sensors* **2012**, *12*, 12347. [Crossref]
26. *GraphPad Prism*, version 6; GraphPad Software Inc., San Diego, USA, 2012.
27. Gomes, R. F.; Lima, L. R. M.; Feitosa, J. P. A.; Paula, H. C. B.; de Paula, R. C. M.; *Int. J. Biol. Macromol.* **2020**, *156*, 446. [Crossref]
28. Lamichhane, S.; Anderson, J.; Remund, T.; Kelly, P.; Mani, G.; *J. Biomed. Mater. Res., Part B* **2015**, *104*, 1416. [Crossref]
29. Abreu, C. M. W. S.; Paula, H. C. B.; Seabra, V.; Feitosa, J. P. A.; Sarmento, B.; de Paula, R. C. M.; *Carbohydr. Polym*. **2016**, *154*, 77. [Crossref]
30. Zhang, K.; Brendler, E.; Geissler, A.; Fischer, S.; *Polymer* **2011**, *52*, 26. [Crossref]
31. Luo, Y.; Yu, W.; Xu, F.; Zhang, L.-L.; *Polym. Chem.* **2012**, *50*, 2053. [Crossref]
32. Safakas, K.; Saravanou, S. F.; Iatridi, Z.; Tsitsilianis, C.; *Int. J. Mol. Sci.* **2021**, *22*, 3824. [Crossref]
33. Khosa, A.; Reddi, S.; Saha, R. N.; *Biomed. Pharmacother.* **2018**, *103*, 598. [Crossref]
34. Feng, H.; Sun, Y.; Zhang, J.; Deng, L.; Dong, A.; *J. Drug Delivery Sci. Technol.* **2018**, *45*, 81. [Crossref]
35. Horie, M.; Fujita, K.; *Adv. Mol. Toxicol*. **2011**, *5*, 145. [Crossref]
36. Dalstein, L.; Haddada, M. B.; Barbillon, G.; Humbert, C.; Tadjeddine, A.; Boujday, S.; Busson, B.; *J. Phys. Chem. C* **2015**, *119*, 17146. [Crossref]
37. Blanco-Fernandes, B.; Concheiro, A.; Makwana, H.; Fernandez-Trillo, F.; Alexander, C.; Alvarez-Lorenzo, C.; *RSC Adv*. **2017**, *7*, 14448. [Crossref]
38. Wang, X.; Cao, W.; Sun, C.; Wang, Y.; Wang, M.; Wu, J.; *Int. J. Pharm.* **2022**, *622*, 121874. [Crossref]
39. Tu, Y.-L.; Wang, C.-C.; Chen, C.-Y.; *J. Polym. Res.* **2018**, *25*, 134. [Crossref]

Submitted: October 3, 2022
Published online: March 15, 2023